

Evaluating Reachable Workspace and User Control Over Prehensor Aperture for a Body-Powered Prosthesis

Alix Chadwell¹, Laurence Kenney¹, David Howard¹, Robert T. Ssekitoleko, *Member, IEEE*, Brenda T. Nakandi, and John Head

Abstract—Using a shoulder harness and control cable, a person can control the opening and closing of a body-powered prosthesis prehensor. In many setups the cable does not pass adjacent to the shoulder joint center allowing shoulder flexion on the prosthetic side to be used for prehensor control. However, this makes cable setup a difficult compromise as prosthesis control is dependent on arm posture; too short and the space within which a person can reach may be unduly restricted, too long and the user may not be able to move their shoulder sufficiently to take up the inevitable slack at some postures and hence have no control over prehensor movement. Despite the fundamental importance of reachable workspace to users, to date there have been no studies in prosthetics on this aspect. Here, a methodology is presented to quantify the reduction in the reachable volume due to the harness, and to record the range-of-motion of the prehensor at a series of locations within the reachable workspace. Ten anatomically intact participants were assessed using a body-powered prosthesis simulator. Data was collected using a 3D motion capture system and an electronic goniometer. The harnessed reachable workspace was 38-85% the size of the unharnessed volume with participants struggling to reach across the body and above the head. Across all arm postures assessed, participants were only able to achieve full prehensor range-of-motion in 9%. The methodologies presented could be used to evaluate future designs of both body-powered and myoelectric prostheses.

Index Terms—Function, harness, prosthetics, range-of-motion, reach, volume, workspace.

I. INTRODUCTION

UPPER-LIMB prostheses can be broadly split into two categories, active and passive. Active prostheses allow

Manuscript received March 2, 2020; revised June 17, 2020; accepted July 16, 2020. Date of publication July 20, 2020; date of current version September 7, 2020. This work was supported by the U.K. Government Global Challenges Research Fund through the Engineering and Physical Sciences Research Council and the National Institute for Health Research under Grant EP/R013985/1. (Corresponding author: *Alix Chadwell*.)

Alix Chadwell, Laurence Kenney, David Howard, and John Head are with the Centre for Health Sciences Research, University of Salford, Salford M5 4WT, U.K. (e-mail: a.e.a.chadwell1@salford.ac.uk; l.p.j.kenney@salford.ac.uk; d.howard@salford.ac.uk; j.head@salford.ac.uk).

Robert T. Ssekitoleko and Brenda T. Nakandi are with the Department of Physiology, Makerere University, Kampala, Uganda (e-mail: rsseki@gmail.com; nakandibrenda95@gmail.com).

Digital Object Identifier 10.1109/TNSRE.2020.3010625

the user to actively control the opening and closing of the prehensor, either through mechanical linkages (known as body-powered devices) or using electric motors.

Where active control is required, upper-limb body-powered prostheses may be particularly suitable for those who undertake manual work and/or do not have access to reliable electricity supplies [1] or those with limited financial resources. Despite this, body-powered prostheses have received very little attention from researchers and have seen little development since the early 20th century [2].

Most body-powered devices use a Bowden cable or a piece of nylon/perlon cord for force transmission. This is attached at the proximal end to a harness (constructed from webbing) worn around the user's shoulders and at the distal end to a lever mechanism in the prehensor, with movement resisted by a spring or elastic band. Dependent on the arrangement of the lever and spring, the user can either voluntarily open or voluntarily close the prehensor. There are several different harness designs [3]; a person with trans-radial (below-elbow) limb absence would most commonly be prescribed a figure-of-8 (Northwestern) harness, or in cases where the prosthesis is self-suspending and the harness is purely for force transmission, a figure-of-9 (P-loop) harness.

As the cable and webbing do not pass adjacent to the centers of rotation for each of the joints, the path length between the axilla loop (the connection between the harness and the contralateral shoulder) and the prehensor is posture dependent. Throughout this paper, we will refer to the 'effective length' of the cable (Fig. 1) defined as follows: 'effective length' is the distance (along the path of the cable) between the most distal connection to the socket (in this study this is the cable lock), and the distal end of the cable (assuming that the cable were not connected to the prehensor and there were no other mechanical stops). When the contralateral shoulder is fully retracted the 'effective length' will be at its maximum, and when the shoulder is fully protracted, the 'effective length' will be at its minimum.

The 'effective length' with the shoulder retracted minus the 'effective length' with the shoulder protracted is the 'User's cable RoM' (Range-of-Motion), which is the maximum possible cable excursion (at the distal end) due to the abduction and adduction of the contralateral shoulder. Conversely, the 'Mechanical cable RoM' is the cable excursion required

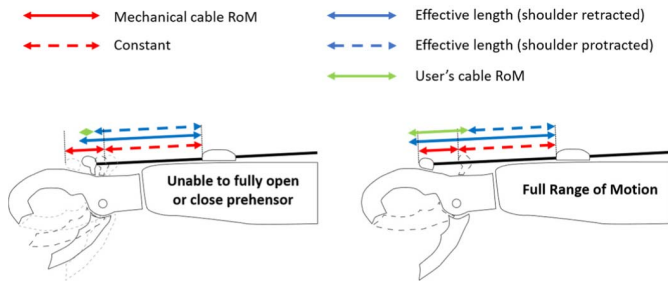


Fig. 1. Effective cable length. For a user to operate the prehensor, the ‘User’s cable RoM’ (the difference between the ‘effective length’ with shoulder retracted and with shoulder protracted) must overlap with the ‘Mechanical cable RoM’. Where only partial overlap occurs, operation will be limited. Where no overlap exists, the user will be unable to operate the prehensor at all.

to fully open and close the prehensor. For the user to operate the prehensor, the ‘User’s cable RoM’ must overlap with the ‘Mechanical cable RoM’ (Fig. 1) and the degree of overlap varies with arm posture.

The setup of the harness system will impact both reachable workspace [4] and the ‘User’s cable RoM’. Increasing the ‘effective length’ during setup, to increase the size of the reachable workspace, could negatively impact on the overlap between the ‘User’s cable RoM’ and the ‘Mechanical cable RoM’ so that the user cannot fully close a voluntary closing terminal device in some arm postures. Conversely, decreasing the ‘effective length’ during setup, to ensure full closure is always possible, could prevent the user from fully opening the device in some arm postures, and from reaching certain parts of the workspace. In other upper-limb impairments, reduced workspace has been shown to have a negative correlation with quality of life [5].

To reflect the need to find a compromise setup for the harness system, a number of clinical guidelines have been developed. These recommend setting the ‘effective length’ whilst the contralateral shoulder is in a neutral position and the prosthetic arm is placed in specified postures; however, these guidelines vary and are somewhat vaguely worded. Further, whether any of the resulting ‘effective lengths’ are optimal in any formal sense is not known. Additionally, many prosthetists will rely on their own (often rather limited) experience of prescribing body-powered devices when setting up the harness system. These factors likely lead to a wide variety of setups in clinical practice, and it is not known what the most common setups are. The New York Upper Limb Prosthetics Manual suggests that full ‘Mechanical cable RoM’ should be achievable at the mouth, the perineum, and at 90 degrees of elbow flexion [6]. The guidelines provided by TRS Prosthetics suggest that, for a voluntary opening device, the ‘effective length’ should be equal to the ‘Mechanical cable RoM’ plus the ‘constant’ (Fig. 1) (i.e. cable ‘just tensioned’) when the arm is hung by the side, and that a voluntary closing device should be 1/3 closed when the arm is hung by the side [7]. An Ottobock video on harness system setup agrees with the aforementioned TRS guidelines for the setup of a voluntary opening prehensor, although in their example the elbow is



Fig. 2. TRS body-powered prosthesis simulator. Please note that these images were taken during pilot testing and as such contain additional markers not used in the final analysis.

slightly flexed [8] and it is unclear from the video whether that is the maximal amount of elbow extension achievable by the user due to the socket design and anatomical restrictions.

In summary, the harness system design and setup limit both where the user can reach and where they can fully activate the prehensor. The extent of these limitations and the implications on function have not been explored. Until we have methods to quantify these limitations, design and setup decisions that influence the ‘effective length’ in different postures will be difficult to justify. Further, methods for quantifying reachable workspace and position dependent variations in a ‘User’s cable RoM’ could be used to evaluate future harness-controlled devices. Therefore, the aims of this proof-of-concept study were to develop suitable methods with which to quantify the limitations on both reachable workspace and the ability to fully exploit the ‘Mechanical cable RoM’ of the prehensor within this space.

II. METHODS

A. Participants

Ten healthy anatomically intact adults with no upper-limb musculoskeletal injuries/abnormalities age (19-49) were recruited from the students at the University of Salford. Ethical approval for the study was granted by the University of Salford Health Research Ethics committee (REF: HSR1819-050) and informed consent was gained from all participants.

B. Equipment

The body-powered prosthesis simulator (TRS Inc), consisted of a wrist brace to be worn on the right arm, a figure-of-9 control harness with a Northwestern style metal ring, and a Bowden cable (Fig. 2). The terminal device was a TRS Voluntary Closing GRIP3 prehensor. This setup is the only commercially available body-powered simulator for use with anatomically intact participants.

Motion data from body-worn and prosthesis-mounted reflective markers were captured at 100Hz using a 13 Oqus camera system (Qualisys, Gothenburg, Sweden).

An electronic goniometer (SG75, Biometrics Ltd) was attached across the mobile ‘thumb’ of the prehensor to measure prehensor aperture (opening and closing). Only one axis for movement around the hinge was recorded. The goniometer was connected to the computer via an adaptor (T9545) and sensor isolator (ST9405AM) developed by Thought Technology Ltd. and data was logged at 100Hz using an Arduino Leonardo (for more details see [9] and Appendix 2 of [10]).

Video recordings were also taken to aid interpretation of the data.

C. Harness Setup

Pilot testing suggested that the guidance offered by the New York Upper Limb Prosthetics Manual was impossible to implement with the TRS system (full ‘Mechanical cable RoM’ should be achievable at the mouth, the perineum and at 90 degrees of elbow flexion [6]). Additionally, for some participants, using the TRS recommended setup (prehensor 1/3 closed when the arm is hung by the side [7]) led to the ‘effective length’ with the contralateral shoulder fully retracted being too short to allow sufficient flexion of the elbow to reach the mouth.

For this study, we undertook pilot testing to develop a setup procedure based on two criteria: (1) Some overlap between the ‘User’s cable RoM’ and the ‘Mechanical cable RoM’ at the mouth was important and (2) We wanted to maximize the data obtained from the study without using different setups, which would have been too time consuming/tiring. We note that for locations where partial overlap between the ‘User’s cable RoM’ and the ‘Mechanical cable RoM’ is achievable, it is possible to predict the required increase or decrease in ‘effective length’ that would be needed to achieve full overlap (full control over hand opening and closing). Conversely, in positions where the subject had no overlap, no inferences could be made on the change needed to achieve full overlap. Therefore, to better interpret the results and predict the effect, at a given posture, of changing the ‘effective length’, it was important that some overlap between the ‘User’s cable RoM’ and the ‘Mechanical cable RoM’ was achievable in all of the arm postures assessed.

Specifically, participants were asked to place their right anatomical hand by their mouth with their shoulders in a neutral, comfortable position (N.B. the anatomical hand was placed in this position rather than the prehensor, which artificially extends the length of the forearm). The harness was then tightened to a point where the tips of the prehensor just met (‘effective length’ equal to the ‘constant’ in Fig. 1); so that, by retracting the contralateral shoulder, the participants could achieve some amount of prehensor opening. Further, if the arm was placed in a different posture where the harness became slack (‘effective length’ increased), by protracting the shoulder some level of closing could still be achieved.

D. Protocol for Data Collection

To measure the trunk position and orientation, a triangular cluster of three markers were placed on the sternum with the top marker (sternum origin) placed at the top of the manubrium just below the jugular notch. To capture the position of the prehensor a marker was placed at its distal end on the fixed of the two ‘jaws’ (herein referred to as the ‘finger’ marker). An additional marker was worn on the acromion of the right shoulder.

Prior to commencing the main part of the study, each participant was invited to stand stationary while 10 seconds of marker data were collected, first while standing upright with

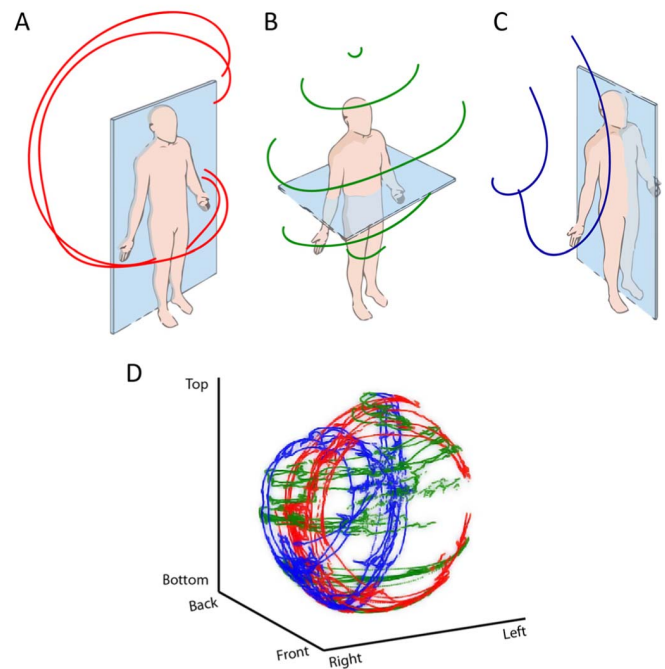


Fig. 3. To calculate the reachable volume, the arm was swept through 9 predefined arcs in the (A) frontal, (B) transverse, and (C) sagittal planes. (D) By combining the data from all of the arc sweeps, a 3D point cloud of fingertip positions was generated.

the arms hung down by their side (Static_{Arm_Down}); second, while standing upright with their right arm held out horizontally to the side (Static_{Arm_Out}) (Note these measurements were undertaken without the harness connected).

1) *Reachable Workspace*: To assess the impact of the harness on the reachable workspace, participants attempted a series of arm sweeps around the body under two conditions: unharnessed and harnessed. In the unharnessed condition, the simulator was still worn but without the harness system (to ensure the same artificially extended forearm length in both conditions). In the harnessed condition, the harness was setup according to the guidelines above.

To capture the reachable workspace, participants were asked to sweep their hand through 9 arcs with the elbow fully extended (note that the contralateral (left) shoulder remained in a neutral position throughout). These arcs were parallel to the frontal, sagittal, and transverse planes as follows:

Frontal (Fig. 3A): 2 arcs were swept around the body in the frontal plane: (1) passing in front of the head and pelvis; and (2) passing behind the head and pelvis.

Transverse (Fig. 3B): 5 arcs were swept across the body in the transverse plane: (1) directly upwards (an arc around the head); (2) with the arm 45 degrees above the horizontal; (3) at shoulder height; (4), with the arm 45 degrees below the horizontal; and (5) directly downwards (an arc around the thighs).

Sagittal (Fig. 3C): 2 arcs were swept parallel to the sagittal plane: (1) in line with the shoulder; and (2) 45 degrees to the side.

Each arc sweep was attempted three times, with the arm in each of three different forearm orientations, corresponding to

the palm facing medially, ventrally, and dorsally. If the starting position for an arc sweep was unachievable, the participant moved onto the next arc. Before attempting each arc sweep, participants were instructed to reach as far away from the body as possible; and during the sweep at approximately 45° intervals they were reminded to extend the arm to maximize reach. When the right shoulder reached its anatomical limit, if the elbow axis of rotation was perpendicular to the motion path, participants were permitted to flex the elbow to extend the sweep until the elbow also met an anatomical limit (or the harness restricted any further movement); at which point the participant was instructed to end the sweep and return to the starting position. During each attempt participants were instructed not to internally or externally rotate their shoulder to get past anatomical limits.

2) *Control Over Prehensor Aperture*: The next part of the experiment was to evaluate the extent to which the participant could open and close the prehensor within their reachable workspace. Whilst holding the prehensor in a range of pre-specified locations around the body, participants were asked to open and close it as far as possible by only abducting and adducting the contralateral (left) shoulder. At each location the participant was given three attempts to open/close the prehensor. They were asked to keep their left hand by their hip during the testing period to reduce compensatory movements of the contralateral shoulder.

E. Data Analysis

1) *Processing the 3D Marker Coordinates*: Data analysis was undertaken using Matlab (Mathworks Ltd). The 3D co-ordinates of the 5 markers were exported from the Qualisys software as a .mat file (note that no filtering or gap filling algorithms were applied within Qualisys). Within Matlab, the 3D co-ordinates were filtered using a 2nd order zero-lag Butterworth filter with a cutoff frequency of 6Hz.

To calculate the workspace with respect to the sternum, all data points were rotated and translated from the lab co-ordinate frame into a sternum co-ordinate frame whose origin was the top sternum marker and whose axes were defined based on the three sternum cluster markers. Fig. 4A. shows the sternum co-ordinate frame and lab co-ordinate frame relative to the participant.

Due to the convex shape of the chest wall, the sternum co-ordinate frame is naturally tilted slightly with respect to the lab frame. To aid visualization a single constant rotation was applied to the results to map from the sternum frame into a corrected sternum co-ordinate frame whose Z-axis was aligned with the Z-axis of the lab coordinate frame (vertical) as shown in Fig. 4B.

Full details of these rotations are reported in the Appendix.

2) *Calculating the Volume of the Reachable Workspace*: For the unharnessed and harnessed conditions, a convex hull (Fig. 5A) surrounding all of the 3D co-ordinates from the ‘finger’ marker and the sternum origin marker was generated using the Matlab alpha shape function. However, for most participants the resulting convex hull enclosed a region formed by joining points at the extremes of the arc sweeps, behind

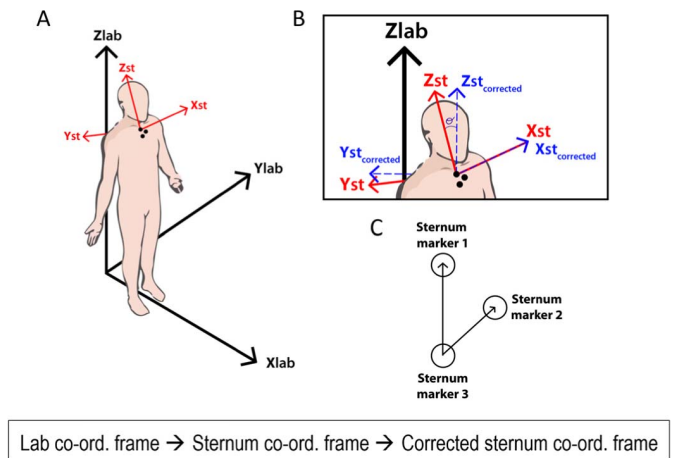


Fig. 4. (A) Orientation of the lab co-ordinate frame and sternum co-ordinate frame relative to the participant. (B) Orientation of the corrected sternum co-ordinate frame relative to the sternum co-ordinate frame. (C) Sternum cluster markers and vectors for calculation of the rotation matrices (See appendix for full description of calculations).

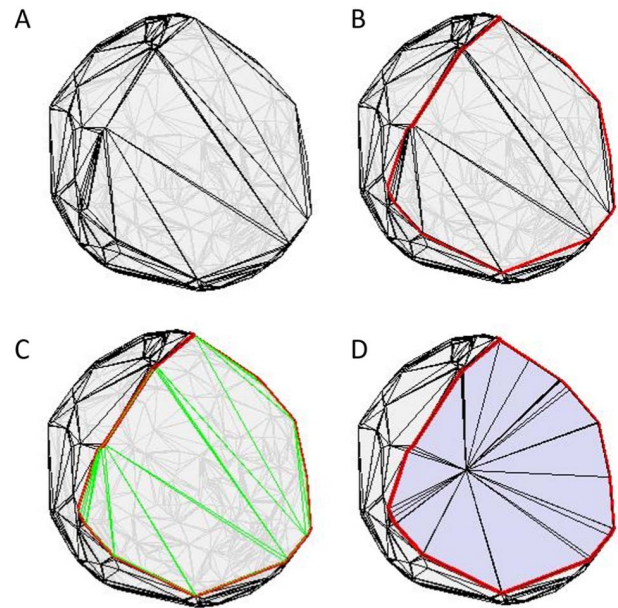


Fig. 5. (A) Convex hull surrounding point cloud of ‘finger’ and sternum positions throughout all arc sweeps, as viewed from behind the person. (B) The facet borders corresponding to the perimeter of the reachable workspace are highlighted in red. (C) The facets that are outside the reachable workspace (joining nodes behind the back) are highlighted in green. These facets are removed from the convex hull. (D) New facets are added joining the perimeter nodes to the sternum.

the back of the participant, while excluding the sternum origin (see Fig. 6 for a simplified 2D explanation). This region was not actually reachable, therefore overestimating the reachable volume. To address this, this region was manually removed as follows.

The convex hull surface triangulation was overlaid over the 3D ‘finger’ co-ordinate point cloud for all of the sweeps. The nodes of the convex hull corresponding to the perimeter joining the extremes of the arc sweeps were manually identified

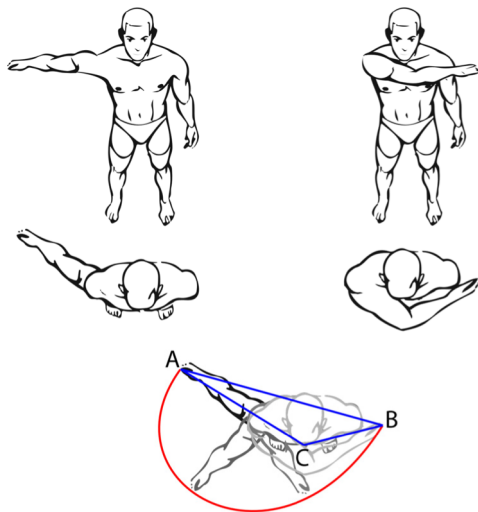


Fig. 6. Simplified 2D example of the overestimation of the workspace due to the convex hull joining the extremes of the sweeps behind the participant's back (point A to point B), but excluding the sternum (point C).

(Fig. 5B and nodes A and B in Fig. 6). Any facets outside of the reachable space were removed (Fig. 5C and facet AB in Fig. 6). Facets were then added to join the perimeter nodes to the sternum origin (Fig. 5D and facets AC and BC in Fig. 6). The volume of the resulting shape was then calculated [11].

3) Quantifying Control Over Prehensor Aperture: The goniometer adaptor output was a voltage between 2.2V and 3.4V, which was digitized, converted to degrees, and filtered in Matlab using a 4th order zero-lag Butterworth filter with a cutoff frequency of 5Hz.

To compensate for changes in alignment between the goniometer and the moving finger joint of the prehensor, between test sessions, the results were normalized to the measured angle change from prehensor fully open to fully closed. When the goniometer was well-aligned, this corresponded to 65° (the prehensor's 'Mechanical aperture RoM').

To simplify the presentation of the data relating to the user's control over prehensor aperture, the arm's workspace was represented by a sphere with its center at the right shoulder marker (Fig. 7A). The location of the right shoulder marker was taken as the mean from the second of the static trials (Static_{Arm_Out}). The radius of the sphere was 6/5 of the participant's arm length, which was defined as the mean distance from the shoulder marker to the finger marker, calculated from the same static trial.

The user's 'Achievable aperture RoM' (in degrees) is presented: (a) trial by trial, i.e. the RoM achieved at a specific hand position and (b) the average RoM achieved for all attempts during which the prehensor sat within a given segment of the aforementioned sphere.

The segments were defined by dividing the sphere as follows (Fig. 7):

- Segments capturing changes in aperture as the arm moves around the body (Fig. 7B). The sphere as viewed from the top was split into eight uniform 45° wedges around the vertical axis (like the segments of an orange).

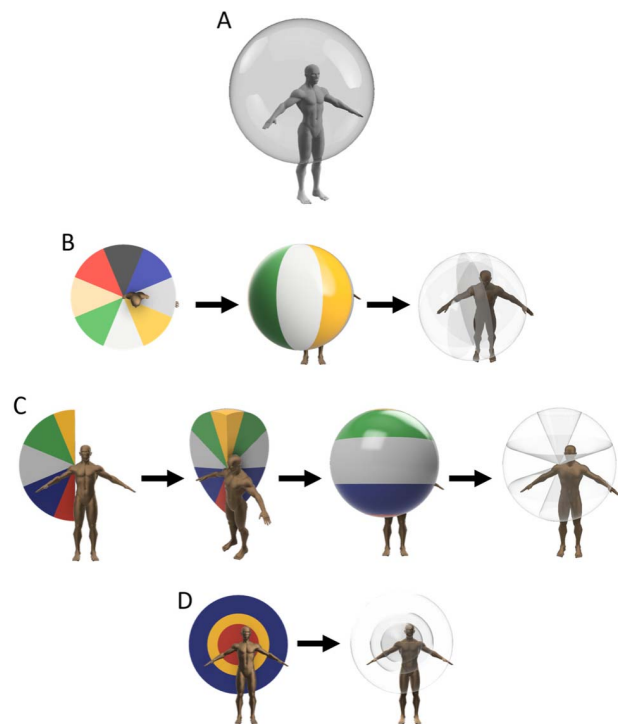


Fig. 7. (A) The arm's workspace was represented by a sphere of radius 6/5 of arm length with its center at the right shoulder. This sphere was subsequently split into vertical, horizontal and radial segments. (B-D) show cross-sectional and 3D views of these segments. (B) Segments capturing changes in aperture as the arm moves around the body: 45° wedges like orange segments, aligned so that if the arm is directly out to the side it falls into the center of a wedge. (C) Segments capturing changes in aperture as the arm moves down the body: 45° sections originating at the center of the sphere and rotated around the vertical axis. (D) Three spherical segments capturing changes in aperture as the arm moves radially away from the body: a) radius < 1/2 arm length; b) 1/2 arm length ≤ radius ≤ 3/4 arm length; c) radius > 3/4 arm length.

- Segments capturing changes in aperture as the arm moves down the body (Fig. 7C). The cross-sectional semi-circle as viewed from the front was split into 5 wedges (3 × 45°, and 2 × 22.5° at the top and bottom); these wedges were rotated around the central vertical axis to create five 3D segments.
- Segments capturing changes in aperture as the arm moves radially away from the body (Fig. 7D). The sphere was split into three spherical segments, referred to as inner (radius < 1/2 arm length), middle (1/2 arm length ≤ radius ≤ 3/4 arm length), and outer (radius > 3/4 arm length). To determine the maximum opening and closing of the prehensor in each trial (i.e. at one prehensor position) and the segment(s) in which this occurs, the following rules were followed:

1. All goniometer data were labelled according to which segment the 'finger' marker was in when the data were recorded (Fig. 8).
2. The peaks (hand as open as possible) and troughs (hand as closed as possible) in the goniometer data were identified using the Matlab *'findpeaks'* function with the Matlab parameter *'minimum peak prominence'* set at 3°. Aperture plateaus were identified as being all contiguous

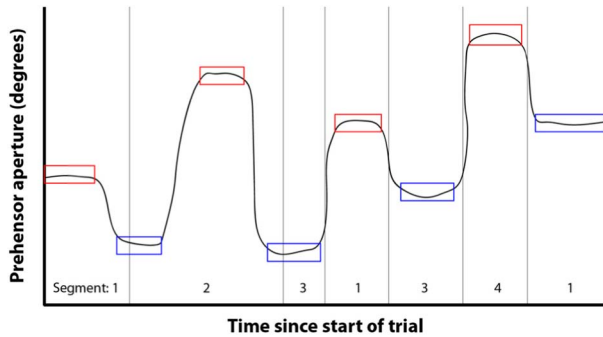


Fig. 8. Artificial goniometer data from one trial. Real data from one trial would usually sit in only one or two segments (in cases where the hand drifts across a boundary line); however, here 4 segments are shown to demonstrate the rules for peak/trough selection. Peak (open) plateaus are identified in red and trough (closed) plateaus are identified in blue. Vertical lines show examples of the 3D ‘finger’ position drifting between segments 1-4.

data within a threshold of -2° from a peak or $+2^\circ$ from a trough (Fig. 8).

3. If any segments did not contain both a peak and a trough, the corresponding plateau data was rejected. For example, in Fig. 8, there was only one peak and no troughs whilst the prehensor was in segment 4, whilst segment 3 only had data from two troughs and no peaks; therefore these data were rejected.
4. Conversely, if the prehensor was in any segment for at least one peak and at least one trough, then the mean aperture for both the maximum (most open) and minimum (most closed) aperture plateaus were labelled as belonging to that segment. For the example shown in Fig. 8, for segment 1 the mean angle from the 5th plateau from the left was recorded as the maximum angle (the value for the 1st plateau being lower) and the mean angle from the 2nd plateau was recorded as the minimum angle (the value for the 8th plateau being higher). Similarly, for segment 2, the mean angle from the 3rd plateau was recorded as the maximum angle and the mean angle from the 4th plateau was recorded as the minimum angle (the value for the 2nd plateau being higher).

III. RESULTS

Marker and goniometer data are published on Figshare [12].

A. Reachable Workspace Volume

Across all ten subjects, the harnessed reachable volume was approximately 70% of the unharnessed volume (Table I). At best there was a 15% reduction in the reachable volume when wearing the harness, and at worst a 62% reduction. Participants 1, 2, and 7 showed the largest reduction ($>50\%$) in reachable volume when wearing the harness. As can be seen in Fig. 9, these three subjects struggled to reach above their shoulders. The volume was restricted for all subjects when bringing the arm across the body as can be seen by the grey sections on the right-hand side of the spheres in Fig. 9.

TABLE I
REACHABLE WORKSPACE VOLUME

Subject No.	Unharnessed volume (m ³)	Harnessed volume (m ³)	Harnessed as a % of unharnessed
1	1.25	0.49	39
2	1.33	0.58	43
3	1.05	0.83	79
4	1.12	0.96	85
5	0.97	0.73	75
6	1.13	1.05	80
7	1.40	0.54	38
8	1.14	0.83	72
9	0.82	0.55	67
10	1.21	0.82	68
Min	0.82	0.49	38
Median	1.18	0.78	70
Max	1.40	1.05	85

B. Evaluation of Control Over Prehensor Aperture

Fig. 10 provides summary plots of ‘Achievable aperture RoM’ for all ten subjects as the hand position moved across the body, down the body, and away from the body. The segment bars are the mean ‘Achievable aperture RoM’, positioned using the mean center point (based on all trials where the prehensor was within that segment). Fig. 11 shows an example of the individual trial RoMs contributing to these mean RoMs for participant 8. The ‘Achievable aperture RoM’ (angular) relates directly to the overlap between the ‘Mechanical cable RoM’ (linear) and the ‘User’s cable RoM’ (linear).

The top row of Fig. 10 shows that all participants found it harder to open the prehensor in postures where the arm was crossed over to the left side of the body as the ‘effective length’ with the contralateral shoulder fully retracted was too short to achieve full opening (harness too tight). Some participants also struggled to close the prehensor when the arm was on the right-hand side of the body as the ‘effective length’ with the contralateral shoulder fully protracted was too long (harness too slack).

The middle row of Fig. 10 shows that, with their arm higher than the sternum all participants found the ‘effective length’ with the contralateral shoulder retracted to be too short (harness too tight) meaning they struggled to open the prehensor. For most participants, as the arm moved down the body, ‘effective length’ with the shoulder retracted and ‘Achievable aperture RoM’ both increased. However, for some the increased slack in the system meant that the ‘effective length’ with the contralateral shoulder fully protracted also increased, making it harder to close the prehensor in the lower segments.

The bottom row of Fig. 10 shows that, when participants operated the prehensor near to their chest, very few were able to open the prehensor beyond 50% aperture (‘effective length’ with contralateral shoulder fully retracted too short). As they extended their arm away from the body, the ‘effective length’ with the shoulder fully retracted generally increased (greater ability to open prehensor), as did the ‘Achievable aperture RoM’.

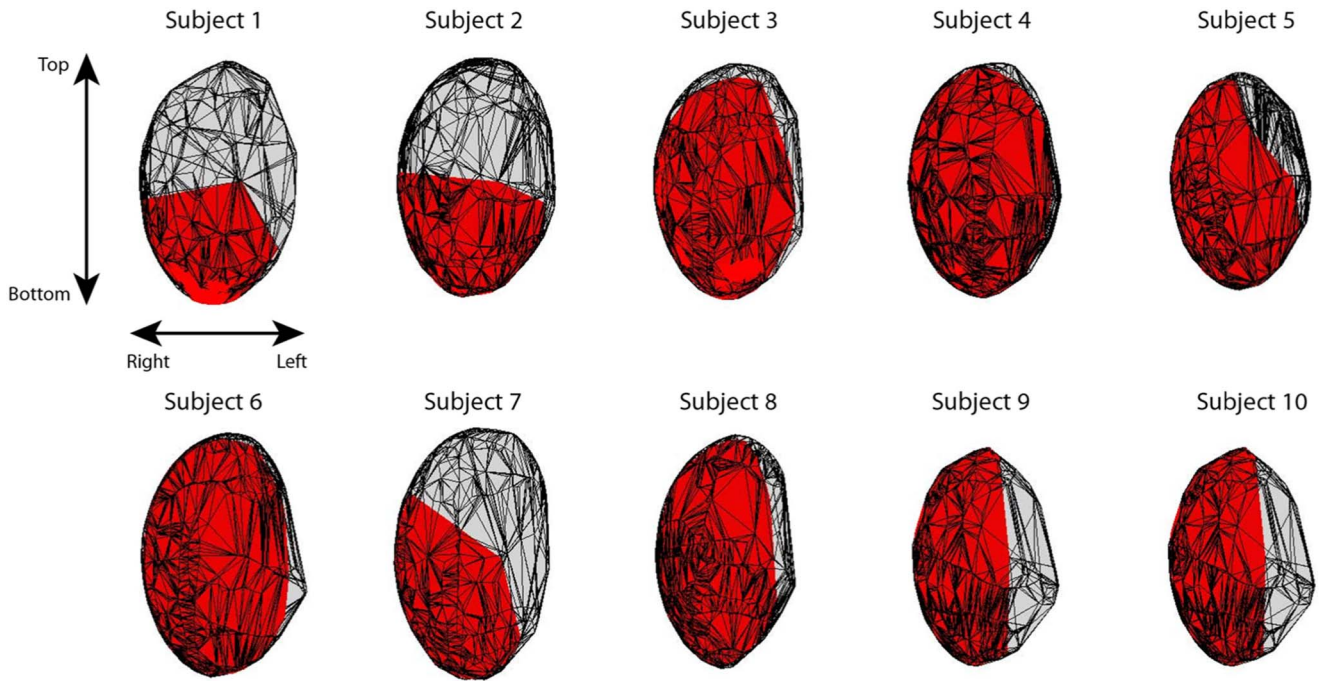


Fig. 9. 3D reachable volume as viewed from the front for all 10 participants. The combined volume shown in both grey and red is the unharnessed reachable volume, and the smaller red sub-volume is the harnessed reachable volume.

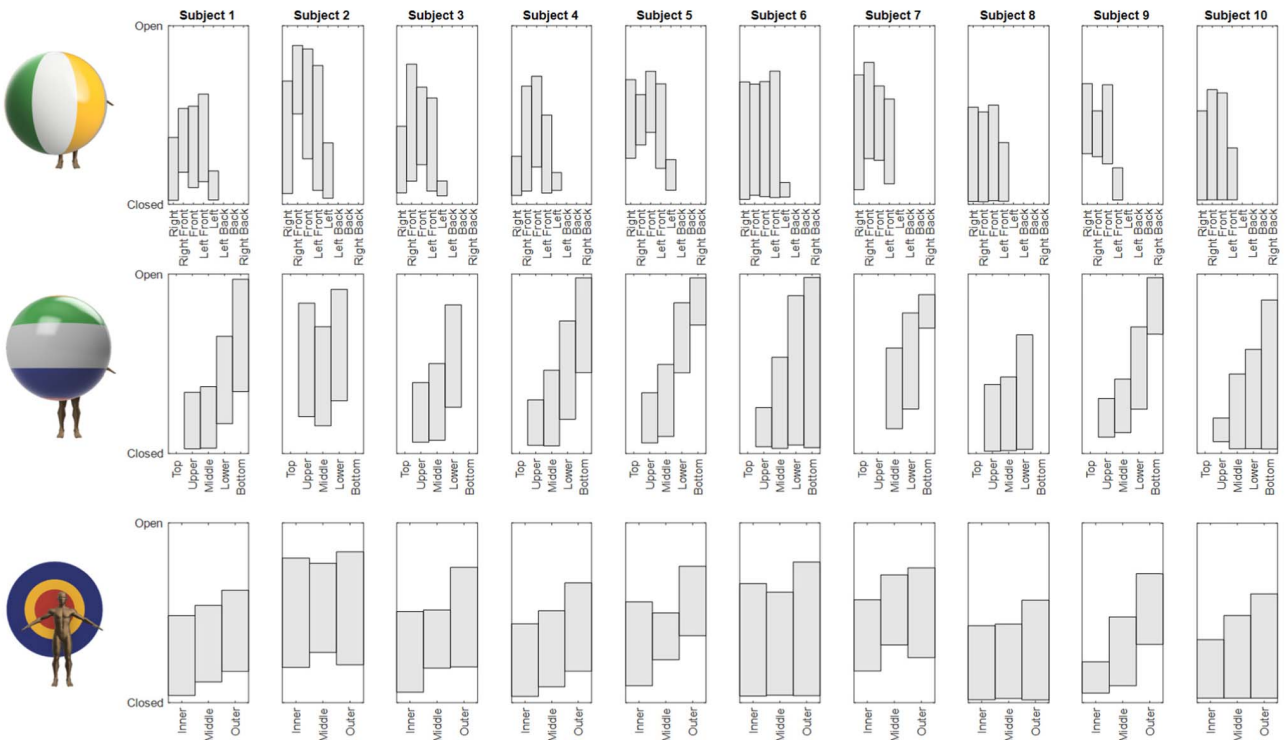


Fig. 10. Summary of user's 'Achievable aperture RoM' (grey bars) for all subjects as the hand moves across the body (top row), down the body (middle row), and away from the body (bottom row). Data presented are mean values recorded across multiple trials. The y-axis limits represent the full 'Mechanical aperture RoM'. See Fig. 11 for an example of the trial data contributing to these mean RoM's.

Across all arm postures assessed for all participants (total 302), participants were only able to achieve the full 'Mechanical aperture RoM' in 27 postures (9%). In 115 postures (38%), the user's 'Achievable aperture RoM' was $\leq 50\%$ of the 'Mechanical aperture RoM'; in 88 of which the

participant struggled to open the prehensor ('effective length' with contralateral shoulder fully retracted too short), and in the other 27 they struggled to close the prehensor ('effective length' with contralateral shoulder fully protracted too long).

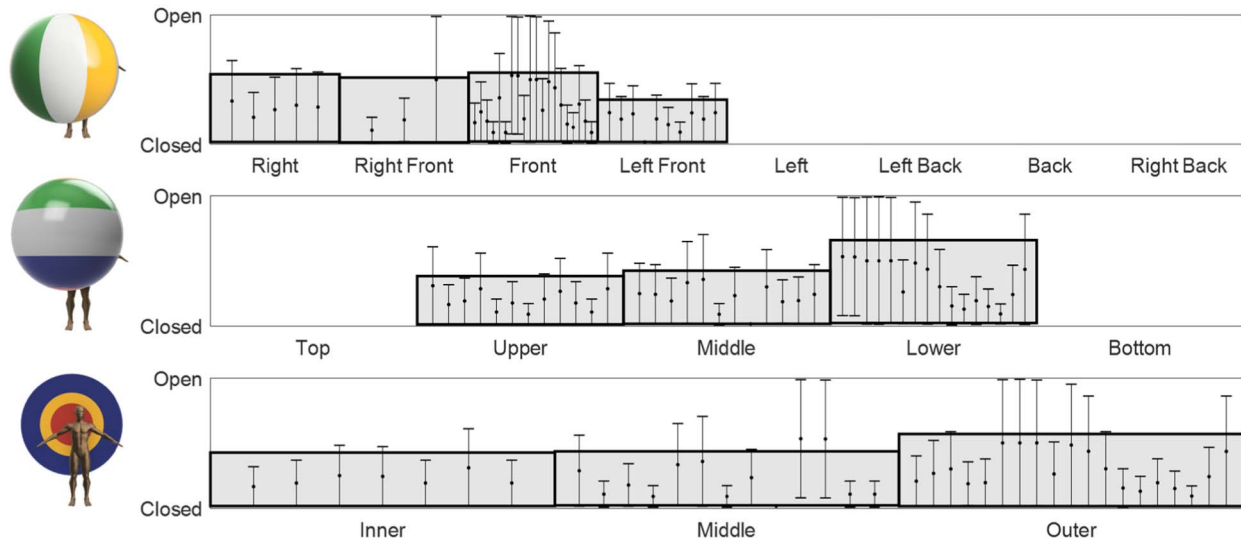


Fig. 11. ‘Achievable aperture RoM’ for participant 8 as the hand moves across the body (top row), down the body (middle row), and away from the body (bottom row). The black lines show the ‘Achievable aperture RoM’ for the individual trials used to calculate the mean RoM and mean RoM center point for each segment (grey bars). The y-axis limits represent the full ‘Mechanical aperture RoM’.

IV. DISCUSSION

This study has introduced novel methods for evaluating reachable workspace and user control over prehensor aperture for a body-powered prosthesis. Clearly, an ‘ideal’ prosthesis would offer the user the ability to position and orient the prehensor at will within his/her unrestricted workspace, and to fully exploit the ‘Mechanical aperture RoM’ anywhere within this volume. The methods introduced here provide an objective approach to evaluating how far a given design is from this ideal.

The commonly used tests of prosthesis and prosthesis user function generally involve performing tasks within a limited subset of the reachable workspace (e.g. SHAP, box and blocks, clothespin relocation test), suggesting the methods presented here complement these approaches.

We chose to study the problem using a structured arc method, variations of which have previously been used in other similar studies [4], [13], to ensure that the end effector was on the workspace boundary. This efficient approach to data collection kept, what was a lengthy protocol for participants, to a minimum. This structured approach also allowed for a repeatable comparison between the two conditions.

The harness system studied imposed major restrictions on where participants could reach. Table I and Fig. 9 show that, when using the harnessed system, participants demonstrated a reduction of between 15% and 62% of their reachable volume compared with the no harness condition. While we do not know how a given reduction in workspace relates to a user’s actual function and satisfaction in daily life, a study of patients recovering from shoulder arthroplasty found a strong correlation between the size of the reachable workspace and patient reported outcome measures such as the Patient-Reported Outcomes Measurement Information System (PROMIS) Physical Function Upper Extremity score and performance on the American Shoulder and Elbow Surgeons (ASES) Standardized Shoulder Assessment Form [5].

Fig. 10 shows that the ability to fully exploit the ‘Mechanical aperture RoM’ in different parts of the reachable workspace is also severely limited by the harness. Out of the 302 arm postures in which aperture RoM was assessed, participants were only able to achieve the full ‘Mechanical aperture RoM’ in 27. For 38% of the measured arm postures, the ‘Achievable aperture RoM’ was $\leq 50\%$ of the ‘Mechanical aperture RoM’. This suggests that the ‘Mechanical aperture RoM’ quoted by manufacturers [14] may provide clinicians and patients with an overly positive view of the functional benefits offered by their device.

Further, it is well established that most body-powered devices, particularly mechanical hands, exhibit poor mechanical efficiency [15], [16]. Hichert found that one consequence of this was that it was not possible for users to generate sufficient grip force without suffering fatigue [17]. Given the number of postures in which full ‘Mechanical aperture RoM’ is not possible, it is likely that users may be frequently coming up against mechanical cable limits in daily life. When the user is up against such a limit, the isometric force generated may be higher than the forces measured by Hichert [17], and consequently the acute risk of fatigue and longer term of overuse injuries may be higher than originally thought.

The general trends in user’s ‘Achievable aperture RoM’ have practical implications for users. Participants found the ‘effective length’ to be too short (cable too tight) when the prehensor was in the upper segments or across the body (to the left-hand side) or too close to the body, and too long (cable too slack) in the lower segments. For a voluntary opening prehensor, this could result in a user being unable to close the prehensor around shirt material when doing up buttons or to close around their harness shoulder strap to adjust it. For a voluntary closing prehensor, they may find themselves crushing their food as they reach towards their mouth or being unable to grasp the material of their trousers. The region in front of the person between their waist and mouth is likely to be the most important area. This region

includes the middle segment (going down the body), and the front right, front, and front left segments (going around the body). Within this region, although all participants were able to close the prehensor, only 3 were able to fully open it, and only one could do so in more than one position. With a voluntary closing prehensor, this would cause issues when trying to grasp large objects. Alternatively, with a voluntary opening prehensor, thin objects may be difficult to grasp. It is worth noting that the mean values presented in Fig. 10 do not tell the whole story, as within each segment, there may be positions where the user can achieve the full ‘Mechanical aperture RoM’ and others where the ‘Achievable aperture RoM’ is very limited (Fig. 11).

Our finding that body-powered prostheses impose restrictions on both reachable workspace and ‘Achievable aperture RoM’ within this space are perhaps unsurprising. Clinicians recognize this to be an issue and hence recommend a number of different approaches to setting the ‘effective length’ of the cable [6]–[8]. It is worth noting that the setup procedure used in this study resulted in a longer ‘effective length’ than the traditional approaches, and as such, these traditional approaches could result in an even greater reduction in reachable workspace, and a greater number of positions where the user achieves $\leq 50\%$ of the full ‘Mechanical aperture RoM’. The methods presented could be used to objectively evaluate alternative setup approaches.

A fundamental issue with many body-powered prostheses is that the control cable does not pass adjacent to the arm joint centers, which means that the ‘Achievable aperture RoM’ is arm posture dependent, affecting both reachable workspace and aperture control. This is particularly the case for the shoulder joint because many harness designs couple shoulder flexion and aperture control. The reason for this is that contralateral shoulder movement alone produces too little cable RoM to satisfy the conflicting requirements of full aperture control and satisfactory grip force. For example, if the ratio between aperture and cable motion is high enough to achieve full ‘Mechanical aperture RoM’ using the contralateral shoulder alone, then the maximum grip force is often too low. One solution would be to incorporate variable mechanical advantage, whereby the ratio changes on grasping an object, which would allow the cable to be rerouted so that the ‘User’s cable RoM’ is no longer arm posture dependent.

It is worth noting that different harness designs may also impact on workspace. In this study, a P-loop harness, constructed using a Northwestern style ring between the Axilla loop and the control strap was used. A P-loop harness may impose particular limitations on workspace closer to the body; other designs such as the figure-of-8 should be evaluated in future work. Our methods could also be used to evaluate other non-harness-based approaches, notably the scapular anchor system [18], and explore the implications of alternative socket designs on workspace. However, it should be noted that simply changing the harness design cannot solve the aperture versus grip force trade-off problem. It is also worth noting that the degree of control over aperture in myoelectric prosthesis users has also been shown to be posture dependent [19] and our techniques could be used to explore this issue in more detail.

In this study we only assessed the outer boundaries of the reachable workspace, suggesting that our findings may be conservative in their estimation of the restrictions imposed by harness-controlled prostheses. In future, it would be recommended to also assess the inner boundaries of the participants reach, providing more detailed information on the restrictions to the workspace close to the body. Although it would seem logical to approach this problem using a variation on the structured arc-based approach to capturing workspace boundaries used here, it may also be worth exploring other, less structured approaches to the data collection protocol. Future studies may also want to consider the automation of the, rather time-consuming process of removing the unreachable volume found using a convex hull-based method. The method reported by Castro *et al.* [20] appears to offer a promising approach.

Finally, to interpret the results of our study and similar future studies there is a need to better understand the implications of a reduced reachable workspace and aperture control limitations for the user’s daily life. The emerging field of real-world monitoring of prosthesis use [21], [22] may offer useful approaches which could be exploited here.

V. CONCLUSIONS

This proof-of-concept study has presented a novel approach to the quantification of a body-powered prosthesis user’s reachable workspace and their ability to exploit the ‘Mechanical aperture RoM’ of the prehensor within that workspace. With the chosen experimental setup, reachable workspace was reduced by between 15 and 62%. Although previous reports have implicitly acknowledged the limitations imposed by current systems, and proposed different approaches to setting up the ‘effective length’ of the cable, this is the first study to quantify the impact on reachable workspace. Further, the study showed, for the first time, that reaching to certain areas around the body is particularly restricted by current setups. The methods presented here could enable future studies to explore the relationship between workspace and more clinical outcomes, building on a study from the shoulder arthroplasty literature [5] which suggests a possible association.

More importantly, the functional advantage associated with wearing the harness (i.e. prehension, via control of aperture) was severely limited by the harness itself. We did not consider the hand orientation in our analysis, but clearly this would also be constrained by the harness, although the available 1 or 2 Degree(s) of Freedom passive wrist units offer a partial solution to this. This is also the first study to report on the extent to which aperture control is restricted by the harness and to show that this effect varies within the reachable workspace. Although different designs of harness and/or different setup procedures may have led to differences in restrictions, the fundamental issue of conflicting design demands on the ratio between aperture and cable motion remains (the ratio should be high to allow for full ‘Mechanical aperture RoM’ and low to achieve sufficient grip force with low cable force). A design in which variable mechanical advantage could be deployed would be worth consideration.

In the shorter term, future studies in prosthesis user cohorts would be recommended. Further, studies to explore the

relationships between reachable and functional workspaces and real-world wear and use (and rejection) would help to understand the importance of different parts of the workspace on everyday function.

APPENDIX

Here the rotation matrix to translate the marker positions from the lab co-ordinate frame into the sternum co-ordinate frame will be described, followed by the calculation of the sternum correction angle.

Unit vectors were generated to represent the sternum X, Y, and Z axes. The Z-axis was defined by the unit vector aligned with sternum markers 3 and 1 (Fig. 4C). The Y-axis unit vector was then the cross product between this vector and the vector between markers 3 and 2 (Fig. 4C). Finally, the X-axis unit vector was the cross product between the sternum Y and Z axes. These unit vectors were used to generate a rotation matrix for each frame (timepoint) and applied to all the marker data in that frame, mapping the marker (x, y z) co-ordinates from the lab co-ordinate frame into the sternum co-ordinate frame.

When calculating the sternum correction angle, the angle of tilt to the left/right of the body was expected to be minimal; therefore the correction angle only considered the mean angle of tilt of the sternum around the sternum X-axis (Fig. 4B). For each frame of the static trial (StaticArm_Down), the unit vector representing the Z axis of the lab (vertical) was rotated into the sternum co-ordinate frame. Then the angle of tilt (ϑ), was calculated as the inverse tangent of the y-co-ordinate of this translated z axis, divided by the z-co-ordinate (See equation 1).

$$\vartheta = \tan^{-1} \left(\frac{{}^{st}Z_{lab y}}{{}^{st}Z_{lab z}} \right) \quad (1)$$

This was averaged across all frames of the static trial (StaticArm_Down) and used to define the constant rotation matrix used to map 3D co-ordinate data from the sternum co-ordinate frame into the corrected sternum co-ordinate frame, see equation (2). This constant rotation based on the mean value of ϑ was applied to every timepoint. In this manuscript, all data are presented in the corrected sternum frame.

$$Corrected_{st} R_{st} = \begin{bmatrix} 1 & 0 & 0 \\ 0 & \cos\vartheta & -\sin\vartheta \\ 0 & \sin\vartheta & \cos\vartheta \end{bmatrix} \quad (2)$$

ACKNOWLEDGMENT

The authors would like to acknowledge the support of Matt Pearson (University of Salford) and Zoe Karthaus (Technical University Delft) in the preparation of the 3D motion capture data. They would also like to thank Peter Kyberd (University of Portsmouth) for his useful inputs regarding the future uses of these measures.

REFERENCES

[1] L. P. J. Kenney *et al.*, "Prosthetics services in Uganda: A series of studies to inform the design of a low cost, but fit-for-purpose, body-powered prosthesis," in *Proc. GReAT Consult.*, Geneva, Switzerland, 2019, pp. 414–426. [Online]. Available: <https://apps.who.int/iris/bitstream/handle/10665/330372/9789240000261-eng.pdf>

[2] N. A. Hashim, N. A. A. Razak, N. A. A. Osman, and H. Gholizadeh, "Improvement on upper limb body-powered prostheses (1921–2016): A systematic review," *Proc. Inst. Mech. Eng., H, J. Eng. Med.*, vol. 232, no. 1, pp. 3–11, Jan. 2018, doi: [10.1177/0954411917744585](https://doi.org/10.1177/0954411917744585).

[3] R. J. Pursley, "Harness patterns for upper-extremity Prostheses," *Artif. Limbs*, vol. 2, no. 3, pp. 26–60, Sep. 1955.

[4] G. Kurillo, A. Chen, R. Bajcsy, and J. J. Han, "Evaluation of upper extremity reachable workspace using kinect camera," *Technol. Health Care*, vol. 21, no. 6, pp. 641–656, Nov. 2013, doi: [10.3233/THC-130764](https://doi.org/10.3233/THC-130764).

[5] A. Ngan *et al.*, "Functional workspace and patient-reported outcomes improve after reverse and total shoulder arthroplasty," *J. Shoulder Elbow Surg.*, vol. 28, no. 11, pp. 2121–2127, Nov. 2019, doi: [10.1016/j.jse.2019.03.029](https://doi.org/10.1016/j.jse.2019.03.029).

[6] *Checkout of Below-Elbow Prostheses, Upper-Limb Prosthetics*, Post-Graduate Med. School Prosthetics Orthotics, New York Univ., New York, NY, USA, 1979.

[7] *TRS Prosthetic Simulator Instructions*. Accessed: Dec. 9, 2019. [Online]. Available: <https://www.trsprosthetics.com/wp-content/uploads/2018/02/Simulator-Instructions.pdf>

[8] *Adjustments of Transradial Body Harness—YouTube*. Accessed: Dec. 9, 2019. [Online]. Available: <https://www.youtube.com/watch?v=uaXP7A2DLik>

[9] A. Chadwell, L. Kenney, S. Thies, A. Galpin, and J. Head, "The reality of myoelectric prostheses: Understanding what makes these devices difficult for some users to control," *Frontiers Neurobotics*, vol. 10, pp. 1–21, Aug. 2016, doi: [10.3389/fnbot.2016.00007](https://doi.org/10.3389/fnbot.2016.00007).

[10] A. E. A. Chadwell, "The reality of myoelectric prostheses: How do EMG skill, unpredictability of prosthesis response, and delays impact on user functionality and everyday prosthesis use?" Ph.D. dissertation, School Health Soc., Univ. Salford, Salford, U.K., 2018. [Online]. Available: <http://usir.salford.ac.uk/id/eprint/47264>

[11] *Volume of a Surface Triangulation—File Exchange—MATLAB Central*. Accessed: Dec. 9, 2019. [Online]. Available: <https://uk.mathworks.com/matlabcentral/fileexchange/26982-volume-of-a-surface-triangulation>

[12] A. Chadwell, "Evaluating reachable workspace and user control over prehensor aperture for a body-powered prosthesis: Data descriptor," Figshare, Univ. Salford, Salford, U.K., Tech. Rep., Jun. 2020, doi: [10.17866/rd.salford.c.5016002](https://doi.org/10.17866/rd.salford.c.5016002).

[13] J. J. Han, G. Kurillo, R. T. Abresch, E. de Bie, A. Nicorici, and R. Bajcsy, "Reachable workspace in facioscapulohumeral muscular dystrophy (FSHD) by kinect," *Muscle Nerve*, vol. 51, no. 2, pp. 168–175, Feb. 2015, doi: [10.1002/mus.24287](https://doi.org/10.1002/mus.24287).

[14] *TRS Product Catalog*. Accessed: Mar. 2, 2020. [Online]. Available: <https://www.trsprosthetics.com/wp-content/uploads/2020/02/TRS-Catalog-2020-compressed.pdf>

[15] G. Smit and D. H. Plettenburg, "Efficiency of voluntary closing hand and hook prostheses," *Prosthetics Orthotics Int.*, vol. 34, no. 4, pp. 27–411, Dec. 2010, doi: [10.3109/03093646.2010.486390](https://doi.org/10.3109/03093646.2010.486390).

[16] G. Smit, R. M. Bongers, C. K. Van Der Sluis, and D. H. Plettenburg, "Efficiency of voluntary opening hand and hook prosthetic devices: 24 years of development?" *J. Rehabil. Res. Develop.*, vol. 49, no. 4, pp. 523–534, 2012, doi: [10.1682/JRRD.2011.07.0125](https://doi.org/10.1682/JRRD.2011.07.0125).

[17] M. Hichert, A. N. Vardy, and D. Plettenburg, "Fatigue-free operation of most body-powered prostheses not feasible for majority of users with trans-radial deficiency," *Prosthetics Orthotics Int.*, vol. 42, no. 1, pp. 84–92, Feb. 2018, doi: [10.1177/0309364617708651](https://doi.org/10.1177/0309364617708651).

[18] M. Hichert and D. H. Plettenburg, "Ipsilateral scapular cutaneous anchor system: An alternative for the harness in body-powered upper-limb prostheses," *Prosthetics Orthotics Int.*, vol. 42, no. 1, pp. 101–106, Feb. 2018, doi: [10.1177/0309364617691624](https://doi.org/10.1177/0309364617691624).

[19] C. Cipriani *et al.*, "Online myoelectric control of a dexterous hand prosthesis by transradial amputees," *IEEE Trans. Neural Syst. Rehabil. Eng.*, vol. 19, no. 3, pp. 260–270, Jun. 2011, doi: [10.1109/TNSRE.2011.2108667](https://doi.org/10.1109/TNSRE.2011.2108667).

[20] M. N. Castro, J. Rasmussen, S. Bai, and M. S. Andersen, "The reachable 3-D workspace volume is a measure of payload and body-mass-index: A quasi-static kinetic assessment," *Appl. Ergonom.*, vol. 75, pp. 108–119, Feb. 2019, doi: [10.1016/j.apergo.2018.09.010](https://doi.org/10.1016/j.apergo.2018.09.010).

[21] A. Chadwell, L. Kenney, M. Granat, S. Thies, J. S. Head, and A. Galpin, "Visualisation of upper limb activity using spirals: A new approach to the assessment of daily prosthesis usage," *Prosthetics Orthotics Int.*, vol. 42, no. 1, pp. 37–44, Feb. 2018, doi: [10.1177/0309364617706751](https://doi.org/10.1177/0309364617706751).

[22] A. Chadwell *et al.*, "Upper limb activity in myoelectric prosthesis users is biased towards the intact limb and appears unrelated to goal-directed task performance," *Sci. Rep.*, vol. 8, no. 1, pp. 1–12, Jul. 2018, doi: [10.1038/s41598-018-29503-6](https://doi.org/10.1038/s41598-018-29503-6).